Journal of Zhejiang University SCIENCE A
ISSN 1673-565X (Print); ISSN 1862-1775 (Online)
www.zju.edu.cn/jzus; www.springerlink.com
E-mail: jzus@zju.edu.cn

Effects of overburden, rock strength and pillar width on the safety of a three-parallel-hole tunnel

Shong-loong CHEN[1], Guo-wei LI[2], Meen-wah GUI[†‡1]

([1]*Department of Civil Engineering, National Taipei University of Technology, Taipei*)

([2]*Department of Civil Engineering, National Chiao-Tung University, Hsinchu*)

[†]E-mail: mwgui@ntut.edu.tw

Received Jan. 16, 2009; Revision accepted May 7, 2009; Crosschecked Sept. 10, 2009

Abstract: During the excavation of three-parallel-hole tunnel, the tunnel might collapse due to over-stress as a result of inadequate rock pillar width. Treating the rock overburden depth, rock strength, and rock pillar width as variables, a series of 3D numerical analysis was carried out to examine the effect of each variable on the safety of the tunnel, in particular the rock pillar. A stress strength ratio (SSR) was used to define whether the safety of the rock pillar was exceeded. A simple design chart for the case of three-parallel-hole tunnel, which took into account the influence of overburden depth, rock pillar width, and rock strength, was also proposed for used in the preliminary design stage.

Key words: Three-parallel-hole tunnel, Tunnels interaction, Rock pillar, Numerical analysis, Stress strength ratio (SSR)
doi:10.1631/jzus.A0920040 **Document code:** A **CLC number:** TU4

INTRODUCTION

Taiwan is a mountainous island with little plains; and developments in the metropolitan areas have resulted in the construction of transportation network, such as the expressway spreading toward the hilly areas. Consequently, a big portion of the expressway requires tunneling through the mountainous terrains. Most of the expressway tunnels in Taiwan are designed as two-parallel-hole tunnels, while some of the long tunnels are designed as three-parallel-hole tunnels with a pilot tunnel running between the two main tunnels (TANEEB, 1991). During the excavation of the tunnel in the rock formation, the stress state of the rock mass, initially in equilibrium, is redistributed through the deformation of the surrounding rock pillar and rock mass and the supporting rock mass lining. In a multi-hole tunnel construction, the pilot tunnel is subjected to stress redistribution because of the main tunnels excavation, which leads to a secondary deformation in the rock mass surrounding the tunnels and in the rock pillars between the tunnels. If the rock pillar width is insufficient, it is possible that the tunnels would fail under tangential uniaxial stress. 2D effects of rock pillar width on the excavation behavior of parallel tunnels were studied by Chen *et al*.(2009), however, the geometry and behavior of rock bolts and anchors can not be truly represented in a 2D analysis.

As technology advances, the performance of computer improves vastly. The popularity of 3D analysis using various numerical tools is now easily available. In this study, a 3D numerical analysis program was deployed to simulate the excavation and construction of the three-parallel-hole Xueshan Tunnel and to investigate the interaction behavior of the tunnels before and after such excavation.

The 12.9-km long Xueshan Tunnel, which is the fifth longest road tunnel in the world and the longest in Southeast Asia, consists of two main tunnels and one pilot tunnel and penetrates through the Xueshan Mountain Range with complex geology and topog-

[‡] Corresponding author

raphy. There were six major faults along the tunnel alignment together with numerous fractures and the rock masses of the mountain were classified from class II to class VI. At its deepest point the tunnel measures 750 m below the surface and the three frequently encountered overburden depths along the tunnel alignment were 100, 250, and 625 m. Reader may refer to Chen *et al.*(2009) for more details on the background of the Xueshan Tunnel.

As a result, a total of 36 numbers of 3D analyses are conducted. The effects of rock overburden depths (100, 250 and 625 m), rock strength based on rock mass classification (classes II, IV and VI) and rock pillar widths (0.5*B*, 1*B*, 2*B* and 4*B*, where *B* is the sum of the radius of the pilot and the main tunnels) on the safety of rock pillar during and after tunnel excavation are discussed.

NUMERICAL MODELING

Finite element mesh

The mesh created was generally similar to the mesh as shown in Fig.1, with the exemption of the upper block. Fig.1a is specifically meant for the case with an overburden depth of 625 m, where the mesh was divided into upper and lower portions. The upper block was used to reduce the number of mesh elements, and hence, the calculation time. This was done by simply assigning a much heavier unit weight to it so that the tunnels would have an overburden stress that is equivalent to an overburden of 625 m. The parameters of the upper block were essentially similar to those shown in Table 1, except that its dry and wet unit weights were 885.5 and 962.5 kN/m^3, respectively. The dimension of the bottom block mesh was 400 m wide, 290 m high and 21.6 m thick. The centers of the pilot and two main tunnels were located at (0, −5, 0), (−13, 0, 0) and (13, 0, 0), respectively. The pilot tunnel used was a four-arc horseshoe shape tunnel with a radius of approximately 2.5 m, whereas the main tunnel was a three-arc horseshoe shape tunnel with a radius of approximately 6 m.

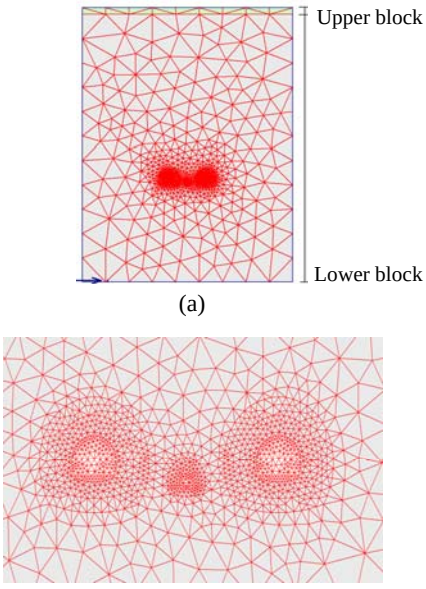

(a)

(b)

Fig.1 (a) Mesh for the 625 m overburden tunnel model; (b) density of grid around the three tunnels

As for the boundary conditions, horizontal displacement was prevented at the four vertical planes of the model while both the vertical and horizontal displacements were prevented at the base of the model. The top boundary was a free boundary.

Table 1 Parameters for classes II, IV and VI rock mass (TANEEB, 1991)

Parameter	Rock mass type		
	II	IV	VI
Dry density (kN/m^3)	23	23	23
Wet density (kN/m^3)	25	25	25
Young's modulus (kPa)	3.0E6	1.2E6	5.0E5
Poisson's ratio	0.25	0.25	0.30
Cohesion (kPa)	1000	300	100
Friction angle (°)	35	30	25
Dilation angle (°)	0	0	0
Tension cut off (kPa)	200	60	20
Stress release rate of rock mass (%)	85	75	65

Materials parameter

The rock mass materials were assumed to be homogeneous and isotropic and their hardness can be identifiable using the geological strength index (Hoek and Brown, 1997). The parameters for rock mass classes II, IV and VI used in the following analysis are shown in Table 1. The value of the stress release rate of rock mass in Table 1 was taken to be less than 1.0 (Brinkgreve and Vermer, 1998).

In addition, the formula representing the relationship between the isotropic coefficient of lateral earth pressure k_o and overburden depth was obtained from Kuang and Wang (1993) who performed inverse analysis on the data of 180 tunnels throughout the

eastern and central parts of Taiwan. Their isotropic coefficient of lateral earth pressure is

$$k_o = 2.0H^{-0.0986}, \quad (1)$$

where H is the overburden depth.

As the topography and geological conditions were complicated and difficult to assess, groundwater table was excluded in the current analysis. In addition, the effect of rock mass creeping was not considered as this parameter was not available. The constitutive model used to represent the rock mass was elastic-perfectly plastic with Mohr-Coulomb failure criterion. Non-associated flow rule was employed with a built-in dilation angle, which means that there was no plastic volumetric expansion behavior after the material failed under constant shear stress.

The support systems adopted in this study were rock anchor and shotcrete. The parameters for the rock anchor and shotcrete adopted for both the pilot and main tunnels in the rock mass classes II, IV and VI are given in Tables 2 and 3, respectively. The rock anchor is made from reinforcement bar of 25 mm in diameter with a Young's modulus of 250 GPa. The shotcrete has compression strength of 21 MPa, and its Young's modulus was determined from $15000\sqrt{f_c} = 21.74$ GPa, where f_c is the compression strength of the shotcrete. The analysis did not consider the primary support sets of the steel ribs and rock bolts.

Plate elements were used to represent the tunnel lining while anchor elements (node-to-node members) were used to represent the rock anchors, hence only axial forces were modeled in the anchors, and no bending moment or friction force was obtained. The reason why such anchor element was still employed was that the pre-tension force could be applied to such element.

Table 2 Parameters for rock anchors (for all pillar widths)

	Parameter	Rock mass type		
		II	IV	VI
Main tunnel	Crowning rock anchor length (m)	N/A	5	5
	Side wall rock anchor length (m)	N/A	9	9
	Young's modulus (kPa)	N/A	2.5E8	2.5E8
	Normal stiffness (kN)	N/A	1.2E5	1.2E5
	Pre-tension (kN)	N/A	98.1	98.1
Pilot tunnel	Rock anchor length (m)	N/A	3	3
	Young's modulus (kPa)	N/A	2.5E8	2.5E8
	Normal stiffness (kN)	N/A	1.2E5	1.2E5
	Pre-tension (kN)	N/A	98.1	98.1

N/A: not applicable

Table 3 Parameters for shotcrete

	Parameter	Rock mass type		
		II	IV	VI
Main tunnel	Shotcrete thickness (m)	0.15	0.20	0.25
	Young's modulus (kPa)	2.1E7	2.1E7	2.1E7
	Normal stiffness (kN/m)	3.15E6	4.2E6	5.25E6
	Flexible stiffness (kN·m^2/m)	5906	14000	27344
	Unit weight (kN·m/m)	3.6	4.8	6.0
	Poisson's ratio	0.17	0.17	0.17
Pilot tunnel	Shotcrete thickness (m)	0.10	0.15	0.20
	Young's modulus (kPa)	2.1E7	2.1E7	2.1E7
	Normal stiffness (kN/m)	2.1E6	3.15E6	4.2E6
	Flexible stiffness (kN·m^2/m)	1750	5906	14000
	Unit weight (kN·m/m)	2.4	3.6	4.8
	Poisson's ratio	0.17	0.17	0.17

Modeling procedures

Although the final results for comparison in this study were taken when all the three tunnels are holed through, in which a 2D plane strain analysis is also acceptable, the geometry and behavior of rock bolts and anchors cannot be truly represented in such a 2D analysis. As a result this study used the commercial program PLAXIS 3D-Tunnel (Brinkgreve *et al.*, 2005) for the following parametric study.

Tunnel excavation commenced immediately after the model achieved its initial stress state. The excavation sequence is denoted in Fig.2. The pilot tunnel was excavated in 2 stages: the upper and lower halves of the cross section; and the left and the right main tunnels were excavated in 3 stages: crown, bench, and invert (Fig.2a). For the main tunnel excavation in classes II, IV and VI rock masses there were 2 steps in every bench: the first was the tunnel excavation and the second was the lining and rock anchors installation (Figs.2b and 2c). Table 1 shows the stress release rates used in the analysis. The second step followed as soon as the forces and displacements reached equilibrium.

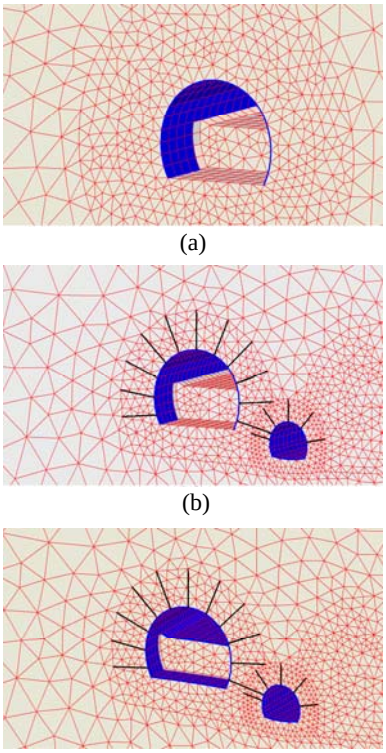

(a) (b) (c)

Fig.2 Bench excavation of main tunnel in (a) class II, (b) class IV and (c) class VI rock masses

The advancing step (distance) for the 3D analysis was 1.6 m in class II rock mass, 1.2 m in class IV rock mass and 0.8 m in class VI rock mass. In addition, for every step advanced, the previous step was strutted. Because class II rock mass has higher strength than classes IV and VI rock masses, thus only shotcrete was used in its support system (Fig.2a). As class IV rock mass has a lower strength than class II rock mass, both the shotcrete and rock anchors were used for its support system (Fig.2b). Since class VI rock mass was the weakest among the three rock masses, shotcrete, rock anchors, and temporary crowning were provided in the excavation of the upper cross section of the pilot and main tunnels (Fig.2c). In addition, a 10 m temporary crowning was provided during the bench excavation of the main tunnel.

RESULTS AND DISCUSSION

The results of the three-parallel-hole tunnel analysis, obtained from a series of Plaxis 3D-Tunnel version 2.0 modeling, are presented and discussed.

Stress strength ratio (SSR), which represents the ratio of the maximum in situ deviatoric stress in a rock pillar and the actual material strength at the same point at each step of the tunnel excavation, was used to define the stress state of the rock pillar. The SSR ratio was employed by a few researchers studying tunnel-related problems (e.g., Hakala and Tolppanen, 2003; Shrestha, 2005). The maximum in situ deviatoric stress J can be calculated from

$$J=\left[\frac{1}{6}\left\{(\sigma_1'-\sigma_2')^2+(\sigma_2'-\sigma_3')^2+(\sigma_3'-\sigma_1')^2\right\}\right]^{0.5}, \quad (2)$$

where σ_1', σ_2' and σ_3' are the effective major, intermediate, and minor principal stresses, respectively. The actual material strength can be calculated from

$$\left(\frac{c'}{\tan\phi'}+p'\right)g(\theta), \quad (2)$$

where ϕ' is the angle of shearing resistance, c' is the cohesion intercept, and p' is the mean effective stress taken as

$$p'=\frac{1}{3}(\sigma_1'+\sigma_2'+\sigma_3'), \quad (3)$$

and $g(\theta)$ is effect of Lode angle, which is expressed as (Georgiadis *et al*., 2004)

$$g(\theta)=\frac{\sin\phi'}{\cos\theta+(\sin\theta\sin\phi')/\sqrt{3}}, \quad (4)$$

hence,

$$\mathrm{SSR}=\frac{J}{\left(\frac{c'}{\tan\phi'}+p'\right)g(\theta)}. \quad (5)$$

The initial major principal stress σ_1' can be calculated by multiplying the overburden depth with the material dry density (Table 1). The initial minor principal stress, which is the initial intermediate principal stress, is taken as $\sigma_2'=\sigma_3'=k_o\sigma_1'$, where k_o is calculated from Eq.(1). Hence, the initial p' for overburden depth of 100, 250, and 625 m is 2714, 6365, and 14951 kPa,

respectively. The corresponding initial in situ deviatoric stress for overburden depth of 100, 250, and 625 m is 359, 532, and 499 kPa, respectively.

The value of SSR, calculated from Eq.(6), will range from 0 to 1. The closer it is to 0 the safer the rock pillar is, because it indicates that the deviatoric stress in the rock pillar during an excavation step is small. However, if SSR approaches 1, it means that the deviatoric stress in the rock pillar during an excavation step is close to the material strength, and hence, the rock pillar is in a relatively unsafe stress state. To obtain the deviatoric stress recording points have been installed in all the models. Gauss stress points that displayed the smallest SSR value before tunnel excavation were selected from the left and the right rock pillars, shown as points A and B in Fig.3, as recording points in this study. This is because, if after excavation, the SSR of either point A or B approaches 1 then all the points on that rock pillar must have had achieved an SSR of 1, and hence, failed.

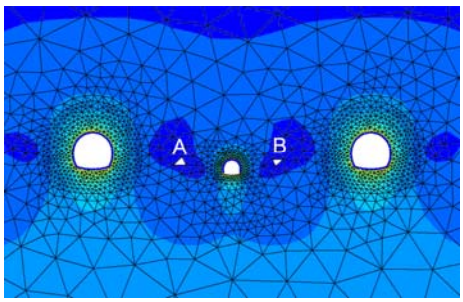

Fig.3 Location of stress recording points A and B

Influence of rock overburden

Three different rock overburden depths: 100, 250 and 625 m for each of the rock mass classification (rock strength), are investigated in this study for their influences on the safety of rock pillar with the widths of 0.5*B*, 1*B*, 2*B* and 4*B*. Here, *B* is the sum of pilot tunnel radius and main tunnel radius. Rock overburden depth affects the in situ vertical stress, and hence, the mean effective stress p' of the rock pillar.

For each pillar width, the smaller the mean effective stress was, the smaller the SSR would be (Fig.4). A smaller mean effective stress corresponded to a shallower rock overburden depth. Therefore, the shallower the overburden is the safer the rock pillar was. Figs.4a~4c also show that, for a particular mean effective stress and rock pillar width, rock pillar made of stronger class II material (Fig.4a) attained a lower SSR value compared to the rock pillar made of weaker class VI material (Fig.4c). The best fitted equations, representing the relationship between SSR and mean effective stresses, were also obtained for the different classes of rock mass in Fig.4.

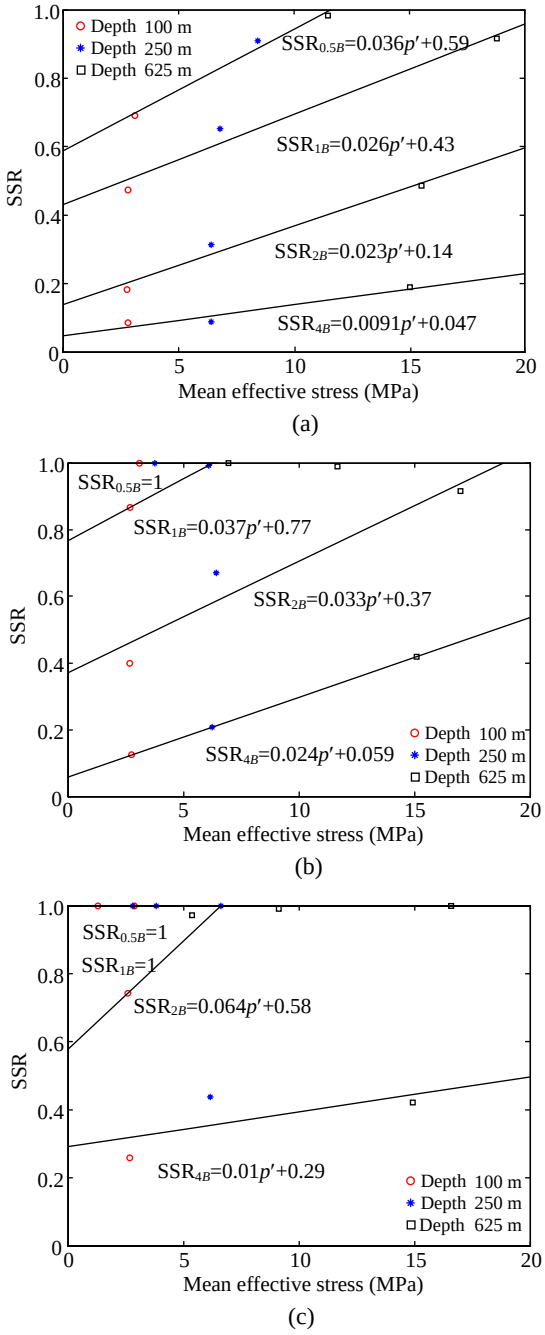

Fig.4 Mean effective stress vs SSR for (a) class II, (b) class IV, and (c) class VI rock masses. Subscript of SSR denotes the rock pillar width, e.g., SSR_{4B} means SSR for rock pillar width 4*B*

Influence of rock strength

Three different rock mass classifications: classes II, IV and VI for each of the overburden depth were investigated here for their influences on the safety of rock pillar with widths of 0.5*B*, 1*B*, 2*B* and 4*B*. The influence of the rock mass classification, in terms of post-excavation rock strength, on the safety of rock pillar could be studied from Fig.5, where the rock post-excavation strength was plotted against SSR.

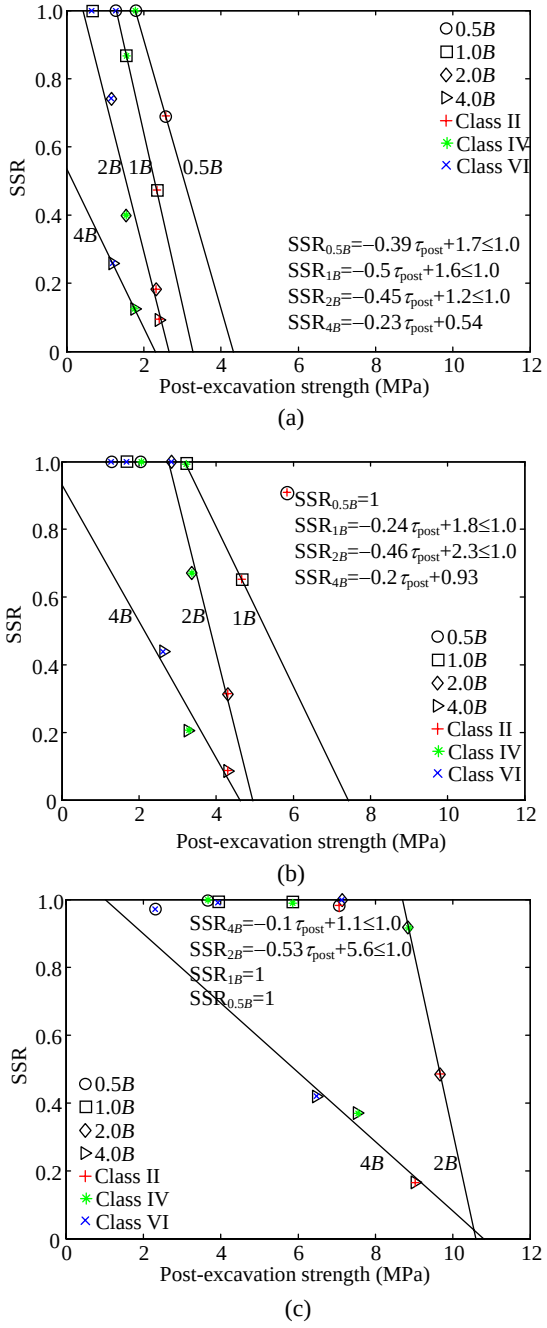

Fig.5 Post-excavation strength (τ_{post}) vs SSR for overburden depth of (a) 100 m, (b) 250 m, and (c) 625 m. Subscript of SSR denotes the rock pillar width, e.g., SSR_{4B} means SSR for rock pillar width 4*B*

For a particular overburden (Fig.5a, 5b and 5c are for overburden depths 100, 250, and 625 m, respectively), a higher post-excavation strength is generally corresponded to a stronger rock mass (class II is stronger than class IV, class IV is stronger than class VI). Take Fig.5a for example, for a particular rock pillar width (take any of the four straight lines), SSR is inversely proportional (straight line with negative gradient) to the post-excavation strength, i.e., the higher the post-excavation strength, the lower the SSR. This implies that, for a particular pillar width, tunneling in class II rock mass is always safer (because SSR is the lowest on this straight line) than tunneling in class VI rock mass (SSR is always the highest on this straight line).

It was also possible to evaluate Fig.5 from the overburden point of view. Fig.5a shows a lower post-excavation strength compared to that shown in Fig.5c; this is because the mean effective stress is lower in Fig.5a (overburden depth=100 m) than that in Fig.5c (overburden depth=625 m) and that from Eq.(3) rock strength is proportional to the mean effective stress. In addition, Fig.5c shows that the SSR values were generally higher than the corresponding ones presented in Fig.5a. This implied that the deeper the overburden depth, the higher the SSR value. The best fitted equations, representing the relationship between SSR and post-excavation strength, were also obtained for the three different overburden depths (100, 250, and 625 m) in Figs.5a~5c, respectively.

Influence of rock pillar width

The influence of rock pillar widths can be studied from Fig.4 or Fig.5. Take Fig.4 for example, it can be seen that the wider the rock pillar width (4*B*), the lower its SSR value. For class II rock mass, even a rock pillar width of 0.5*B* could still be safe for tunneling under an overburden depth of 250 m (Fig.4a). For class VI rock mass, rock pillar widths of 0.5*B* and 1*B* would result in an unsafe tunneling (Fig.4c).

As for Fig.5a, which shows the post-excavation strength versus SSR for an overburden depth of 100 m, rock pillar width of 0.5*B* could only be used in class II rock mass. For classes IV and VI rock masses, one should anticipate an unsafe tunneling work. For rock

pillar width of 2*B*, unsafe tunneling would still occur in class VI rock mass under the overburden depths of 250 and 625 m. For the three overburden depths: 100, 250 and 625 m, it was necessary to use a rock pillar width of 4*B* for all the three different classes of rock mass.

Combined interaction of overburden, rock strength, and rock pillar width

The combined interaction of rock overburden depth (mean effective stress), rock strength and rock pillar width on the safety of a three-parallel-hole tunnel can be studied by normalizing the mean effective stress against the material post-excavation strength, as shown in Fig.6a. For Fig.6a, the horizontal *x*-axis denotes the ratio of "mean effective stress and post-excavation material strength" and the vertical *y*-axis denotes the "rock pillar width". From all the data points plotted on Fig.6a, one could perform interpolation and hence obtain the three straight lines, which represent the SSR of 0.25, 0.5, and 1.0, respectively. Thus, from the three straight line of positive gradient it was observed that the ratio of mean effective stress and post-excavation material strength increases as the ratio of rock pillar width increases.

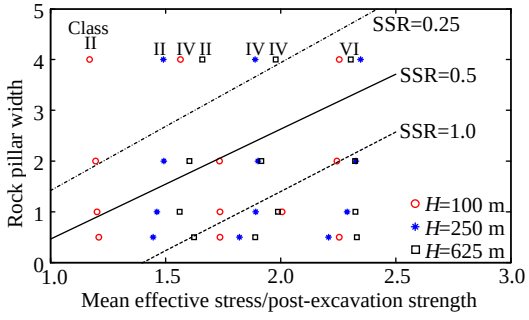

(a)

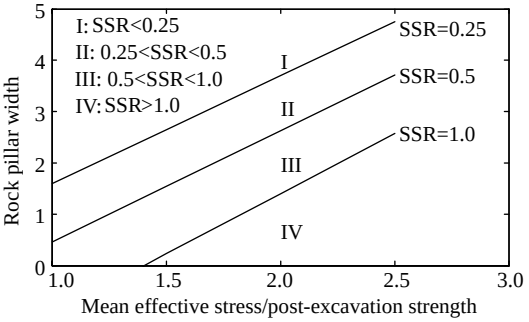

(b)

Fig.6 (a) Ratio of mean effective stress and material strength vs rock pillar width; (b) idealized plot of (a)

Fig.6a could be slightly idealized by making the line representing SSR=0.25 slightly parallel to the other two SSR lines, as shown in Fig.6b. One could then divide Fig.6b into four regions (I~IV), where SSR<0.25, 0.25<SSR<0.5, 0.5<SSR<1.0, and SSR>1.0. This figure could then be used in the initial planning and design of a three-parallel-hole tunnel, providing the information of overburden depth and material strength, together with the design value of the SSR criterion.

It should be noted that Fig.6b only applies to the excavation of three-parallel-hole tunnels with rock overburden depths ranging from 100 to 625 m, classes II through VI rock mass, and rock pillar width between 0.5*B* and 4*B*. In addition, the limitation of Fig.6 is that the influences of the relative sizes between the pilot tunnel and the main tunnels on the safety of the rock pillar have not been taken into account in this study.

CONCLUSION

In this paper, a series of numerical modeling was carried to study the influences of rock overburden depth, rock strength, and rock pillar width on the safety of three-parallel-hole tunnel. The safety of the tunneling was quantified through the introduction of the stress strength ratio SSR. From the study, the following conclusions can be made:

1. Stronger material was always associated with a lower SSR value.

2. Deeper overburden depth was associated with a higher SSR value.

3. In most cases, the wider the rock pillar width was the safer the tunnel would be.

In this study, a normalized plot of the ratio of mean effective stress/material strength versus the ratio of rock pillar width for a specific three-parallel-hole tunnel excavation was suggested. If there is a rock mass undergoing a three-hole tunnel excavation in which the above three parameters dominate, the SSR of the tunnel can be estimated by first calculating the "mean effective stress" from Eq.(4) and then the "material strength" from Eq.(3). Hence, the stress state of the rock pillar can be predicted for the initial stage of the design.

References

Brinkgreve, R.B.J., Broere, W., Waterman, D., 2005. Plaxis 3D-Tunnel, version 2. Delft University of Technology and Plaxis B.V., the Netherlands.

Brinkgreve, R.B.J., Vermer, P.A., 1998. Plaxis, Finite Element Code for Soil and Rock Analyses. A.A. Balkema, Rotterdam, Broodfield.

Chen, S.L., Lee, S.C., Gui, M.W., 2009. Effects of rock pillar width on the excavation behavior of parallel tunnels. *Tunnelling and Underground Space Technology*, **24**(2):148-154. [doi:10.1016/j.tust.2008.05.006]

Georgiadis, K., Potts, D.M., Zdravkovic, L., 2004. Modelling the shear strength of soils in the general stress space. *Computers and Geotechnics*, **31**(5):357-364. [doi:10.1016/j.compgeo.2004.05.002]

Hakala, M., Tolppanen, P., 2003. Analyses of Tunnel Stress Failures at Pyhäsalmi Mine. ISRM–Technology Roadmap for Rock Mechanics, South African Institute of Mining and Metallurgy, p.461-464.

Hoek, E., Brown, E.T., 1997. Practical estimates of rock mass strength. *International Journal of Rock Mechanics and Mining Sciences and Geomechanics Abstracts*, **34**(8):1165-1186. [doi:10.1016/S0148-9062(97)00305-7]

Kuang, P.S., Wang, W.L., 1993. Practical application of FLAC in tunnel engineering. *Sino-Geotechnics*, **41**:53-54 (in Chinese).

Shrestha, G.L., 2005. Stress Induced Problems in Himalayan Tunnels with Special Reference to Squeezing. PhD Thesis, Norwegian University of Science and Technology, Norway, p.203.

TANEEB (Taiwan Area National Expressway Engineering Bureau), 1991. Basic Design of Taipei-Ilan Expressway Project. Final Report of Geological Investigations for Pinlin-Touchen Section (in Chinese).

Wang, W.L., 1993. Practical application of FLAC in tunnel engineering. *Sino-Geotechnics*, **41**:53-54 (in Chinese).